THIRD INTERNATIONAL CONFERENCE ON ADVANCED COMPUTATIONAL METHODS IN ENGINEERING
30 MAY - 2 JUNE 2005, GHENT - BELGIUM
ACOMEN-2005-087

A Nonlinear Discrete-Time Model for Saturated Surface Permanent-Magnet Synchronous Machines

Frederik M.L.L. De Belie*, Jan A.A. Melkebeek,

Lieven Vandevelde, Kristof R. Geldhof, René K. Boel

Department of Electrical Energy, Systems and Automation (EESA)

Ghent University, Sint-Pietersnieuwstraat 41, 9000 Gent, Belgium

Abstract

In this paper a nonlinear discrete-time model for surface permanent-magnet synchronous machines (SPMSM) is given. The novel model takes into account the eddy-current losses, the saturation of the magnetizing flux paths and the magnetic interaction between the two orthogonal magnetic axes. To describe the nonlinear relationship between magnetizing flux and current, a small-signal dynamic flux model is used, derived by differentiating the coenergy. Furthermore, an equivalent electrical circuit is used to model the eddy-current losses and the voltage drop across the stator resistance and leakage inductance. As in most modern drives a digital controller is used, the model is formulated in discrete time. By using a root locus technique the stability of the discrete-time model is discussed.

Keywords: permanent-magnet synchronous machines, saturation, eddy currents, finite element method, root locus technique
AMS classification: 78A25, 65Q05

1 Introduction

Permanent-magnet synchronous machines (PMSM) are an excellent choice for most servo applications. As modern high-grade magnetic materials have a straight line B-H demagnetization characteristic with a high remanent flux density and a high coercitive field, PMSM can have a high energy density. Furthermore, as the magnetic field is generated by using permanent magnets instead of a field winding most of the copper and iron losses appear in the stator. Consequently, cooling of the motor, through the stator, is easily achieved and a small machine inertia and frame size can be realized. Despite these advantages, modern high-grade permanent-magnets can be expensive and a permanent demagnetization of the magnets causes a permanent reduced motor efficiency.
Based on the rotor construction and position of the magnets, different PMSMs can be distinguished. In this paper only PMSMs with magnets mounted on the rotor surface, commonly referred to as surface PMSM or SPMSM, are discussed. As such drives are often used in applications requiring a high-dynamical behaviour, an accurate and fast control or estimation of position, speed or torque is needed. As a result, a dynamical model of a PMSM can be required.

*Corresponding author. E-mail: Frederik.DeBelie@UGent.be.

In this paper a nonlinear discrete-time model is presented. The novel model takes into account the eddy-current losses, the saturation of the magnetizing flux paths and the magnetic interaction between the two orthogonal magnetic axes. To describe the nonlinear relationship between magnetizing flux and current, a small-signal dynamic flux model is used. Such a model is derived by differencing the coenergy calculated by using a finite element method. Furthermore, to model the eddy-current losses and the voltage drop across the stator resistance and leakage inductance, an equivalent electrical circuit is proposed. As in most modern drives a digital controller is used, the model is formulated in discrete time by using a forward rectangular rule. By using a root locus technique the stability of the discrete-time model is discussed.

2 Modelling Electrical Machines

2.1 Stator Voltage Equation

The relationship between stator voltage $\underline{v}_s$, stator current $\underline{i}_s$ and stator flux $\underline{\phi}_s$ is classically described by the stator voltage equation. In a two-dimensional stationary reference frame ($\alpha\beta$) with the real axis along the α-axis, the voltage equation in complex notation is given by

$$\underline{v}_s^{\alpha\beta} = R_s \underline{i}_s^{\alpha\beta} + \frac{\mathrm{d}\underline{\phi}_s^{\alpha\beta}}{\mathrm{dt}}, \tag{2.1}$$

with R_s the stator resistance. Transformation of (2.1) to a complex reference frame (qd), with the real axis fixed to the physical quadrature axis, results in

$$\underline{v}_s^{qd} = R_s \underline{i}_s^{qd} + \frac{\mathrm{d}\underline{\phi}_s^{qd}}{\mathrm{dt}} + j\omega_r \underline{\phi}_s^{qd}, \tag{2.2}$$

with ω_r the angular speed in a stationary reference frame. For small flux variations from steady state, the voltage equation in (2.2) results in

$$\Delta\underline{v}_s^{qd} = R_s \Delta\underline{i}_s^{qd} + \frac{\mathrm{d}\Delta\underline{\phi}_s^{qd}}{\mathrm{dt}} + j\underline{\Phi}_s^{qd}\Delta\omega_r + j\Omega_r \Delta\underline{\phi}_s^{qd}, \tag{2.3}$$

with Δ denoting small variations from steady state and with Ω_r, $\underline{\Phi}_s$ the steady-state values of rotor speed and stator flux respectively corresponding to the operating point. Furthermore, the variation of stator voltage can be written as

$$\Delta\underline{v}_s^{qd} = (\Delta v_s + jV_s\Delta\delta)e^{j\delta_o}, \tag{2.4}$$

with the load angle δ the angle between stator voltage $\underline{v}_s$ and the q-axis and with V_s and δ_o the steady-state values of stator voltage modulus and angle respectively corresponding to the operating point. The relationship between the pulsation ω of the stator voltage in a stationary reference frame, the angular speed ω_r and the load angle δ is given by

$$\frac{\mathrm{d}\delta}{\mathrm{dt}} = \omega - \omega_r, \tag{2.5}$$

which, for small variations, results in

$$\frac{\mathrm{d}\Delta\delta}{\mathrm{dt}} = \Delta\omega - \Delta\omega_r. \tag{2.6}$$

2.2 Nonlinear Magnetic Circuit

From here on we assume that the stator flux $\underline{\phi}_s$ comprises the leakage flux $\underline{\phi}_\sigma$ additionally to the magnetizing flux $\underline{\phi}_m$

$$\underline{\phi}_s^{qd} = \underline{\phi}_\sigma^{qd} + \underline{\phi}_m^{qd}, \tag{2.7}$$

where the leakage flux varies linearly with the stator current

$$\underline{\phi}_\sigma^{qd} = L_\sigma \underline{i}_s^{qd}, \tag{2.8}$$

whereas the relationship between magnetizing flux and current is assumed to be nonlinear. In order to model the main magnetic circuit chord-slope and tangent-slope inductances are defined, derived by differentiating the coenergy. By assuming the magnetic circuit is lossless (or the losses are taken into account separately), the coenergy W_{co} can be expressed as

$$W_{co} = \int (\phi_{mq} \mathrm{d}i_q + \phi_{md} \mathrm{d}i_d), \tag{2.9}$$

where

$$\underline{\phi}_m^{qd} = \phi_{mq} + j\phi_{md} \quad \text{and} \quad \underline{i}^{qd} = i_q + j i_d. \tag{2.10}$$

As a result the flux linkages, for a given current, are given by

$$\phi_{mq}(i_q, i_d) = \frac{\partial W_{co}(i_q, i_d)}{\partial i_q} \quad \text{and} \quad \phi_{md}(i_q, i_d) = \frac{\partial W_{co}(i_q, i_d)}{\partial i_d}. \tag{2.11}$$

Instead of using two variables i_d and i_q, the coenergy can always be written as a function of a magnetizing current $\underline{i}_m^{qd} = \underline{i}_m^{qd}(i_q, i_d)$. From here on we assume that the current $\underline{i}_m^{qd}$ can be written as

$$\underline{i}_m^{qd}(i_q, i_d) = K i_q + j i_d \,, K \in I\!R_o^+. \tag{2.12}$$

Then it follows from (2.11) that

$$\phi_{mq}(i_q, i_d) = \frac{\mathrm{d}W_{co}(i_m^{qd})}{\mathrm{d}i_m^{qd}} \cdot \frac{\partial i_m^{qd}(i_q, i_d)}{\partial i_q} = L_{qo}(i_m^{qd}) \cdot i_q, \tag{2.13}$$

$$\phi_{md}(i_q, i_d) = \frac{\mathrm{d}W_{co}(i_m^{qd})}{\mathrm{d}i_m^{qd}} \cdot \frac{\partial i_m^{qd}(i_q, i_d)}{\partial i_d} = L_{do}(i_m^{qd}) \cdot i_d, \tag{2.14}$$

with L_{qo}, L_{do} the chord-slope inductances. This means that, if the assumption in (2.12) holds, the relationship between flux and current depends on i_m only. Furthermore, the chord-slope inductance for each current can be obtained from the direct and quadrature chord-slope inductances with excitation respectively in the d- and q-axis only [4]. In a dynamical analysis the incremental or tangent-slope inductances are required as well

$$L_{qt}(i_q) = \frac{\mathrm{d}\phi_{mq}(i_q, 0)}{\mathrm{d}i_q} \quad \text{and} \quad L_{dt}(i_d) = \frac{\mathrm{d}\phi_{md}(0, i_d)}{\mathrm{d}i_d}. \tag{2.15}$$

To model the magnetic circuit, the current $\underline{i}^{qd}$ is transformed to a magnetizing current $\underline{i}_m^{qd}$. As a result, the definitions of the inductances in (2.13)-(2.15) are altered

$$L_{qmo}(i_m) = \frac{L_{qo}(i_m)}{K}, \quad L_{dmo}(i_m) = L_{do}(i_m), \quad L_{qmt}(i_{mq}) = \frac{L_{qt}(K i_q)}{K}, \quad L_{dmt}(i_{md}) = L_{dt}(i_d). \tag{2.16}$$

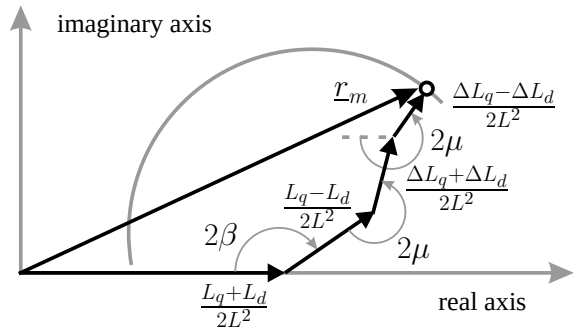

Figure 1: Trajectory of the equivalent reluctance $\underline{r}_m$ of the main magnetic circuit for a circular trajectory of $\Delta\underline{\phi}_m^{qd}$.

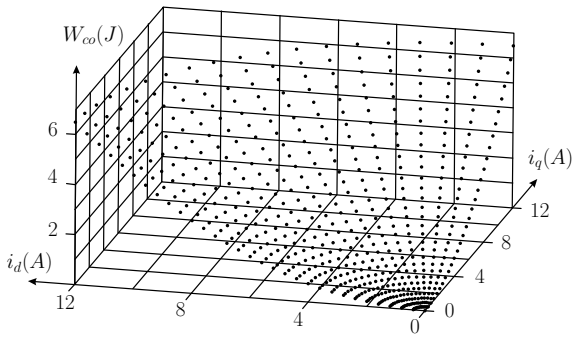

Figure 2: Simulated coenergy for different magnetizing currents, calculated using the finite element method.

2.3 Small Signal Dynamic Flux Model

The relationship between magnetizing flux $\underline{\phi}_m^{qd}$ and magnetizing current $\underline{i}_m^{qd}$ in the proximity of an operating point is described in [3] by using a small signal dynamic flux model. By assuming (2.12), this model is based on inductances as defined in (2.13)-(2.15) and is written in a matrix notation. In [1], this model is given in a complex notation

$$\Delta\underline{i}_m^{qd} = \underline{r}_m \cdot \Delta\underline{\phi}_m^{qd}, \tag{2.17}$$

with the complex magnetizing reluctance $\underline{r}_m$

$$\underline{r}_m = \frac{L_u + \underline{L}_{rel} + \underline{L}_{sat}}{L^2}. \tag{2.18}$$

The inductances in (2.18) are given by

$$L_u = \frac{L_q + L_d}{2}, \tag{2.19}$$

$$\underline{L}_{rel}(\beta) = -\frac{L_q - L_d}{2} e^{-j2\beta}, \tag{2.20}$$

$$\underline{L}_{sat}(\beta,\mu) = \big(-\frac{\Delta L_q - \Delta L_d}{2} + \frac{\Delta L_q + \Delta L_d}{2} e^{-j2\beta} \big) e^{j2\mu}, \tag{2.21}$$

$$L^2 = L_q L_d + (L_q \Delta L_d - L_d \Delta L_q)\cos(2\mu) - \Delta L_q \Delta L_d, \tag{2.22}$$

with

$$L_q = \frac{L_{qmo} + L_{qmt}}{2}, \quad L_d = \frac{L_{dmo} + L_{dmt}}{2}, \quad \Delta L_q = \frac{L_{qmo} - L_{qmt}}{2}, \quad \Delta L_d = \frac{L_{dmo} - L_{dmt}}{2} \tag{2.23}$$

and with β the angle between $\Delta\underline{\phi}_m^{qd}$ and the q-axis, μ the angle between the steady-state magnetizing current $\underline{I}_m^{qd}$ corresponding to the operating point and the q-axis. In a current-controlled drive, the steady-state stator current $\underline{I}_s^{qd}$ and as a consequence the current I_m^{qd} and the angle μ as well, are controlled to a constant value. The proposed small-signal dynamic flux model in (2.17) models the nonlinear magnetic condition and the cross saturation or magnetic interaction between the d- and q-axis. However, the model considers the fundamental space harmonic components only. Thus, in the model fundamental flux variations due to the slotting effect are neglected. Moreover, the saturation of the leakage flux path is neglected as well. In Fig. 1, the complex reluctance $\underline{r}_m$ is given for a variable β. For a given $\underline{I}_m^{qd}$ and an increasing β from $-\pi$ to π the reluctance $\underline{r}_m$ follows a circular trajectory in the complex plane.

2.4 Equation of Motion

By controlling the electromagnetic torque t_{em} the angular speed ω_r can be altered. This relationship is classically modelled by using a first order differential equation

$$\frac{J}{N_p} \cdot \frac{\mathrm{d}\omega_r}{\mathrm{dt}} = t_{em} - t_l, \tag{2.24}$$

with J the inertia of machine and load, N_p the number of pole pairs and t_l the load torque. The torque t_{em} can be written as [5]

$$t_{em} = \frac{3}{2} N_p \Im\big(\underline{\phi}_s^{qd} \cdot \underline{i}_s^{qd*}\big), \tag{2.25}$$

where * denotes the complex conjugate. Assuming the load torque t_l can be written as a linear function of the angular speed ω_r

$$t_l = t_l' + K_w \omega_r, \tag{2.26}$$

the equation of motion (2.24) for small variations from steady state results in

$$\frac{J}{N_p} \cdot \frac{\mathrm{d}\Delta\omega_r}{\mathrm{dt}} = \Delta t_{em} - \Delta t_l' - K_w \Delta\omega_r. \tag{2.27}$$

From (2.25) it follows that the variation of the torque t_{em} can be approximated by

$$\Delta t_{em} = \frac{3}{2} N_p \Im\big(\Delta\underline{\phi}_s^{qd} \cdot \underline{I}_s^{qd*} + \underline{\Phi}_s^{qd} \cdot \Delta\underline{i}_s^{qd*}\big). \tag{2.28}$$

3 Surface Permanent-Magnet Synchronous Machines

3.1 Equivalent Circuit

The previously given model is used to describe the behaviour of a surface PMSM. For such a motor the coenergy is calculated for different currents as is shown in Fig. 2. From this result, it follows that the coenergy can be quite accurately approximated with a function of the magnetizing current $\underline{i}_m$ as defined in (2.12) with K equal to one. This means that, for each magnetizing current,

$$L_{qmo} = L_{dmo} = L_{mo} \quad \text{and} \quad L_{qmt} = L_{dmt} = L_{mt}. \tag{3.29}$$

As a consequence the complex reluctance $\underline{r}_m$ in (2.17) results in

$$\underline{r}_m = R_m\Big(1 + \lambda e^{-j2(\beta-\mu)}\Big), \tag{3.30}$$

where

$$R_m = \frac{2}{L_{mo} + L_{mt}} \quad \text{and} \quad \lambda = \frac{L_{mo} - L_{mt}}{L_{mo} + L_{mt}}. \tag{3.31}$$

The reluctance $\underline{r}_m$ in per unit for a given modulus of $\underline{I}_m^{qd}$, in the case of a surface PMSM, is shown in Fig. 3. It can be seen that the direction of $\underline{I}_m^{qd}$ influences the phase shift between $\Delta\underline{i}_m^{qd}$ and $\Delta\underline{\phi}_m^{qd}$ for the same β. Clearly, the effect of saturation and magnetic interaction between both orthogonal magnetic axes is reflected in $\underline{r}_m$.

The eddy-current losses in a SPMSM are classically modelled as a resistance R_y in parallel with the magnetizing inductance [6]. By using the voltage equation in (2.3), by modelling the magnetic circuit as in (2.17) and by assuming that the eddy-current losses for a surface PMSM are equal in both orthogonal magnetic axes, a novel equivalent circuit is obtained as is shown in Fig. 4. It can be seen that such a circuit models the voltage drop across the stator resistance R_s and leakage inductance L_σ as well.

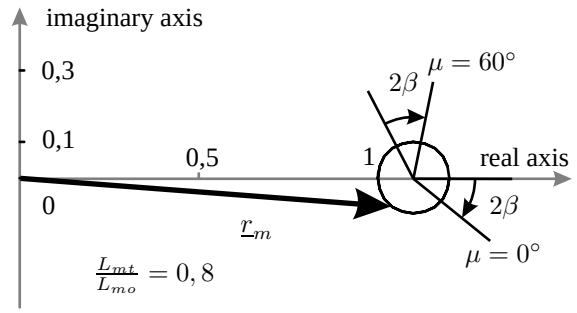

Figure 3: Reluctance $\underline{r}_m$ in per unit with β as parameter in the case of a high magnetizing current for a surface PMSM.

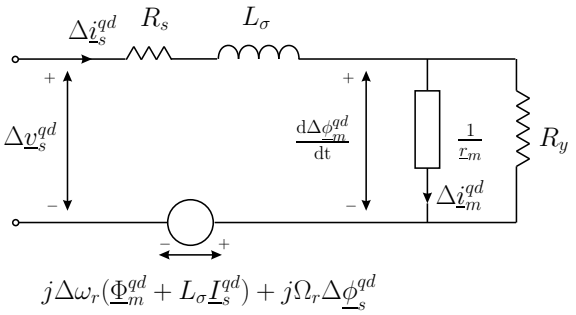

Figure 4: Equivalent circuit for a surface PMSM.

3.2 Small-Signal Difference Equations

As some SPMSM drives use a digital controller, a discrete-time model is required. For this reason, the equations describing the model are discretized in time. By using the forward rectangular rule [2], the relationship, in a discrete time, between stator current and magnetizing flux is given by

$$\Delta \underline{\phi}_m^{qd}(k+1) = T_s R_y \Delta \underline{i}_s^{qd}(k) + T_s \Big(\frac{1}{T_s} - R_y \underline{r}_m(k) \Big) \Delta \underline{\phi}_m^{qd}(k), \tag{3.32}$$

with T_s the time step. The complex inductance in discrete time is obtained by adapting (3.30)

$$\underline{r}_m(k) = R_m \Big(1 + \lambda e^{-j2(\beta(k)-\mu)} \Big). \tag{3.33}$$

From (3.32) and by differencing (2.3) it follows

$$\begin{aligned} \Delta \underline{i}_s^{qd}(k+1) = {} & T_s \Big(- \frac{R_s + R_y}{L_\sigma} + \frac{1}{T_s} - j\Omega_r \Big) \cdot \Delta \underline{i}_s^{qd}(k) \\ & + T_s \Big(\frac{R_y \underline{r}_m(k)}{L_\sigma} - j \frac{\Omega_r}{L_\sigma} \Big) \cdot \Delta \underline{\phi}_m^{qd}(k) \\ & - j T_s \frac{\Phi_s^{qd}}{L_\sigma} \cdot \Delta \omega_r(k) + T_s \frac{1}{L_\sigma} e^{j\delta_o} \cdot \Delta v_s(k) + j T_s \frac{V_s}{L_\sigma} e^{j\delta_o} \cdot \Delta \delta(k). \end{aligned} \tag{3.34}$$

Differencing the equation of motion in (2.27) it follows

$$\begin{aligned} \Delta \omega_r(k+1) = {} & (1 - T_s K_w \frac{N_p}{J}) \Delta \omega_r(k) \\ & + T_s \frac{N_p}{J} \Delta t_{em}(k) - T_s \frac{N_p}{J} \Delta t_l'(k), \end{aligned} \tag{3.35}$$

where, by using (2.28)

$$\Delta t_{em}(k) = \frac{3}{2} N_p \Im \Big(\Delta \underline{\phi}_s^{qd}(k) \cdot \underline{I}_s^{qd*} + \underline{\Phi}_s^{qd} \cdot \Delta \underline{i}_s^{qd*}(k) \Big). \tag{3.36}$$

3.3 Discrete-Time State-Space Model

The difference equations given in (3.32)-(3.36), obtained by a forward rectangular rule, can be written as a state-space discrete-time model. By defining the state $\boldsymbol{X}$ and input $\boldsymbol{U}$ as

$$\boldsymbol{X}(k) = \left[\begin{array}{cccccc} \Delta\phi_{mq}(k) & \Delta\phi_{md}(k) & \Delta i_{sq}(k) & \Delta i_{sd}(k) & \Delta\omega_r(k) & \Delta\delta(k) \end{array} \right]^T, \tag{3.37}$$

$$\boldsymbol{U}(k) = \left[\begin{array}{ccc} \Delta v_s(k) & \Delta t_l'(k) & \Delta\omega(k) \end{array} \right]^T, \tag{3.38}$$

where ^{T} denotes the transposed vector, it follows from (3.32)-(3.36) that

$$\boldsymbol{X}(k+1) = \widetilde{\boldsymbol{A}} \cdot \boldsymbol{X}(k) + \widetilde{\boldsymbol{B}} \cdot \boldsymbol{U}(k), \tag{3.39}$$

with

$$\widetilde{\boldsymbol{A}} = T_s \cdot \left[\begin{array}{cccccc} \frac{1}{T_s} - R_y r_{11} & -R_y r_{12} & R_y & 0 & 0 & 0 \\ -R_y r_{21} & \frac{1}{T_s} - R_y r_{22} & 0 & R_y & 0 & 0 \\ \frac{R_y}{L_\sigma} r_{11} & \frac{R_y}{L_\sigma} r_{12} + \frac{\Omega_r}{L_\sigma} & \frac{1}{T_s} - \frac{R_s + R_y}{L_\sigma} & \Omega_r & \frac{\Phi_{md} + L_\sigma I_{sd}}{L_\sigma} & -\frac{V_{sd}}{L_\sigma} \\ \frac{R_y}{L_\sigma} r_{21} - \frac{\Omega_r}{L_\sigma} & \frac{R_y}{L_\sigma} r_{22} & -\Omega_r & \frac{1}{T_s} - \frac{R_s + R_y}{L_\sigma} & -\frac{\Phi_{mq} + L_\sigma I_{sq}}{L_\sigma} & \frac{V_{sq}}{L_\sigma} \\ \frac{3}{2}\frac{N_p^2}{J} I_{sd} & -\frac{3}{2}\frac{N_p^2}{J} I_{sq} & -\frac{3}{2}\frac{N_p^2}{J}\Phi_{md} & \frac{3}{2}\frac{N_p^2}{J}\Phi_{mq} & \frac{1}{T_s} - K_w\frac{N_p}{J} & 0 \\ 0 & 0 & 0 & 0 & -1 & \frac{1}{T_s} \end{array} \right], \tag{3.40}$$

$$\widetilde{\boldsymbol{B}} = T_s \left[\begin{array}{cccccc} 0 & 0 & \frac{\cos\delta_o}{L_\sigma} & \frac{\sin\delta_o}{L_\sigma} & 0 & 0 \\ 0 & 0 & 0 & 0 & -\frac{N_p}{J} & 0 \\ 0 & 0 & 0 & 0 & 0 & 1 \end{array} \right]^T, \tag{3.41}$$

where

$$\begin{array}{ll} r_{11} = R_m(1 + \lambda\cos(2\mu)), & r_{12} = R_m(1 + \lambda\sin(2\mu)), \\ r_{21} = R_m(1 - \lambda\sin(2\mu)), & r_{22} = R_m(1 - \lambda\cos(2\mu)), \end{array} \tag{3.42}$$

and

$$\underline{V}_s^{qd} = V_{sq} + jV_{sd}, \quad \underline{I}_s^{qd} = I_{sq} + jI_{sd}, \quad \underline{\Phi}_m^{qd} = \Phi_{mq} + j\Phi_{md}, \quad \Delta\underline{i}_s^{qd} = \Delta i_{sq} + j\Delta i_{sd}. \tag{3.43}$$

4 Stability of the Discrete-Time State-Space Model

4.1 Model in Closed-Loop Form

The stability of the novel model in (3.39) can be discussed by using a root locus technique. For this reason, the model is given in a closed-loop form as is shown in Fig. 5 where C denotes the concatenation

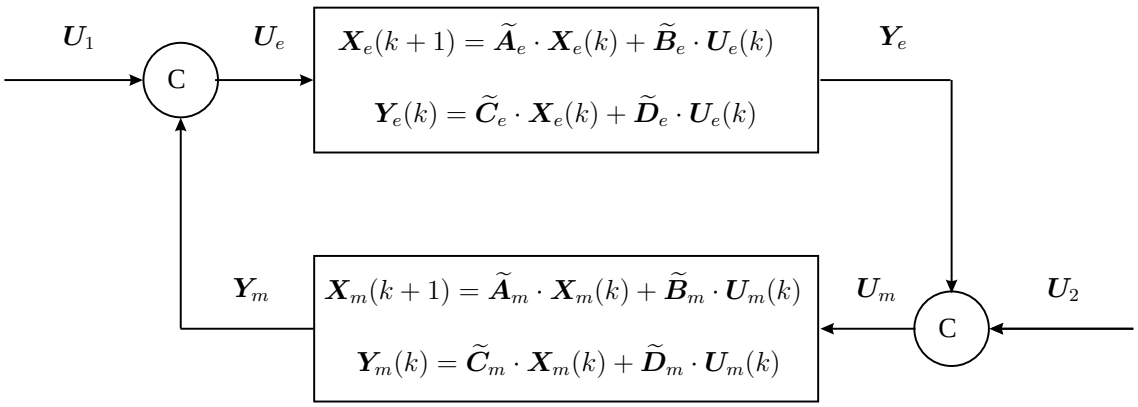

Figure 5: Block diagram of a surface PMSM.

of two vectors. State vector $\boldsymbol{X}_e$, input vector $\boldsymbol{U}_e$ and output vector $\boldsymbol{Y}_e$ for the upper state-space model are defined by

$$\boldsymbol{X}_e(k) = \begin{bmatrix} \Delta\phi_{mq}(k) & \Delta\phi_{md}(k) & \Delta i_{sq}(k) & \Delta i_{sd}(k) \end{bmatrix}^T, \tag{4.44}$$

$$\boldsymbol{U}_e(k) = \begin{bmatrix} \Delta v_s(k) & \Delta i_{rd}(k) & \Delta i_{rq}(k) \end{bmatrix}^T \quad \text{and} \quad \boldsymbol{Y}_e(k) = [\Delta t_{em}(k)]\,. \tag{4.45}$$

The matrices used in this model are given by

$$\widetilde{\boldsymbol{A}}_e = T_s \begin{bmatrix} \frac{1}{T_s} - R_y r_{11} & -R_y r_{12} & R_y & 0 \\ -R_y r_{21} & \frac{1}{T_s} - R_y r_{22} & 0 & R_y \\ \frac{R_y}{L_\sigma} r_{11} & \frac{R_y}{L_\sigma} r_{12} + \frac{\Omega_r}{L_\sigma} & \frac{1}{T_s} - \frac{R_s + R_y}{L_\sigma} & \Omega_r \\ \frac{R_y}{L_\sigma} r_{21} - \frac{\Omega_r}{L_\sigma} & \frac{R_y}{L_\sigma} r_{22} & -\Omega_r & \frac{1}{T_s} - \frac{R_s + R_y}{L_\sigma} \end{bmatrix}, \tag{4.46}$$

$$\widetilde{\boldsymbol{B}}_e = T_s \begin{bmatrix} 0 & 0 & 0 \\ 0 & 0 & 0 \\ \frac{\cos\delta_o}{L_\sigma} & 1 & 0 \\ \frac{\sin\delta_o}{L_\sigma} & 0 & 1 \end{bmatrix}, \tag{4.47}$$

$$\widetilde{\boldsymbol{C}}_e = \frac{3}{2} N_p \begin{bmatrix} I_{sd} & -I_{sq} & -\Phi_{md} & \Phi_{mq} \end{bmatrix} \quad \text{and} \quad \widetilde{\boldsymbol{D}}_e = \begin{bmatrix} 0 & 0 & 0 \end{bmatrix}. \tag{4.48}$$

State vector $\boldsymbol{X}_m$, input vector $\boldsymbol{U}_m$ and output vector $\boldsymbol{Y}_m$ for the lower state-space model are defined by

$$\boldsymbol{X}_m(k) = \begin{bmatrix} \Delta\omega_r(k) & \Delta\delta(k) \end{bmatrix}^T, \quad \boldsymbol{U}_m(k) = \begin{bmatrix} \Delta t_{em}(k) & \Delta t'_l(k) & \Delta\omega(k) \end{bmatrix}^T \tag{4.49}$$

$$\text{and} \quad \boldsymbol{Y}_m(k) = \begin{bmatrix} \Delta i_{rd}(k) & \Delta i_{rq}(k) \end{bmatrix}^T. \tag{4.50}$$

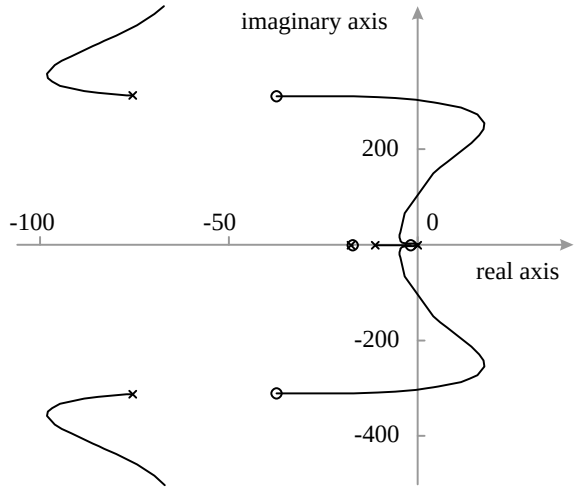

Figure 6: Root locus of the continuous-time model of an unloaded SPMSM at nominal speed.

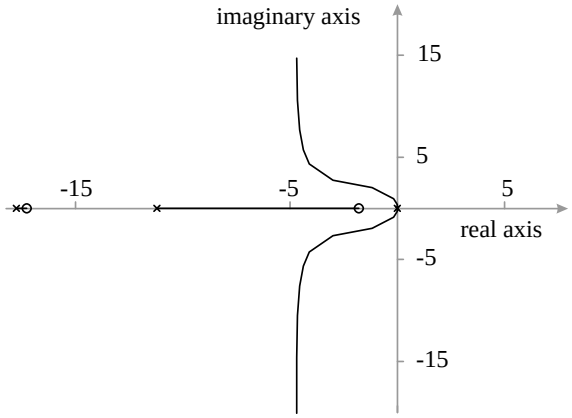

Figure 7: Root locus of the continuous-time model nearby the origin of the s-plane.

The matrices used in this state-space model are given by

$$\widetilde{\boldsymbol{A}}_m = T_s \begin{bmatrix} \frac{1}{T_s} - K_w \frac{N_p}{J} & 0 \\ -1 & \frac{1}{T_s} \end{bmatrix}, \quad \widetilde{\boldsymbol{B}}_m = T_s \begin{bmatrix} \frac{N_p}{J} & -\frac{N_p}{J} & 0 \\ 0 & 0 & 1 \end{bmatrix}, \tag{4.51}$$

$$\widetilde{\boldsymbol{C}}_m = \frac{1}{L_\sigma} \begin{bmatrix} \Phi_{md} + L_\sigma I_{sd} & -V_{sd} \\ -\Phi_{mq} - L_\sigma I_{sq} & V_{sq} \end{bmatrix} \quad \text{and} \quad \widetilde{\boldsymbol{D}}_m = \begin{bmatrix} 0 & 0 & 0 \end{bmatrix}. \tag{4.52}$$

4.2 Root Locus of a Surface PMSM

By using the block diagram in Fig. 5 the root locus of the novel discrete-time model can be calculated. However, to discuss the stability of the discrete-time model, the root locus of the continuous-time model is required as well. Such a model can be obtained in a simular way as the new discrete-time model. The resulting root locus of a continuous-time model for an unloaded SPMSM at nominal speed is given in Fig. 6. Furthermore, in Fig. 7, this root locus is shown in the vicinity of the origin of the s-plane. It can be seen that the system becomes unstable for certain values of the open loop gain. The root locus of the discrete time system is shown in Fig. 8. In Fig. 9, the root locus is shown nearby the origin of the z-plane. It can be seen that, besides the unstable region as mentioned for the continuous-time model, the system becomes unstable from a certain gain as well. As the forward rectangular rule is used, a continuous-time model can be mapped on an unstable discrete-time model [2]. However, by decreasing the time step T_s a higher open-loop gain margin is obtained.

5 Conclusion

In this paper a uniform small-signal dynamic model is presented to describe electrical machines and in particular surface permanent-magnet synchronous machines or SPMSMs. Through differencing the coenergy, obtained from a finite element method, the main flux path can be described by a complex reluctance. As a result the novel model takes into account the saturation of the magnetizing flux paths and the magnetic interaction between the two orthogonal magnetic axes. In the case of a surface PMSM,

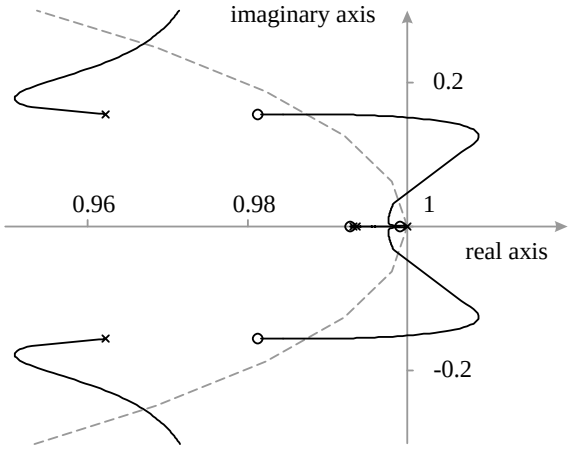

Figure 8: Root locus of the discrete-time model of an unloaded SPMSM at nominal speed.

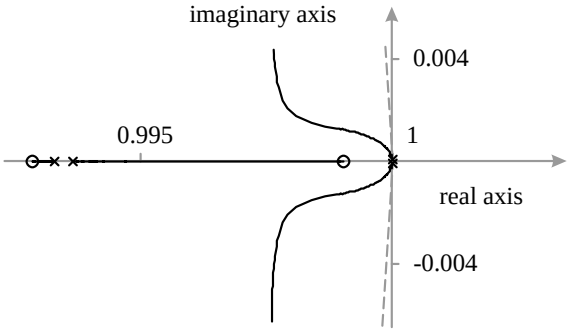

Figure 9: Root locus of the discrete-time model nearby the origin of the z-plane.

an equivalent circuit is presented that includes the eddy-current losses and the voltage drops across stator resistance and leakage inductance. However, the model considers the fundamental space harmonic components only. Thus, in the model fundamental flux variations due to the slotting effect are neglected. Moreover, the saturation of the leakage flux path is neglected as well. The model is transformed to a discrete-time state-space model by using a forward rectangular rule. In this way a prediction of the dynamical behaviour of the machine can be made. By using a root locus technique, the stability of the new model is discussed. For this purpose, the model is given in a closed-loop form as well. From the calculated root locus it is concluded that the stability of a PMSM is only guaranteed for certain values of the open loop gain. Moreover, by using the forward rectangular rule, a well-considered time step has to be chosen.

References

[1] F.M.L.L. De Belie, J.A.A. Melkebeek, K.R. Geldhof, L. Vandevelde and R.K. Boel, A general description of high-frequency position estimators for interior permanent-magnet synchronous motors, *Conf. Proc. Int. Conf. El. Mach. (ICEM)*, Cracow, Poland, 5-8 Sept. 2004, CD-ROM, paper 390.

[2] G.F. Franklin, J.D. Powell and M. Workman, *Digital control of dynamic systems*, (3th ed.), Addison Wesley Longman, California, 1998.

[3] J.A.A. Melkebeek, Small signal dynamic modelling of saturated synchronous machines, *Conf. Proc. Int. Conf. El. Mach. (ICEM)*, Lausanne, Switzerland, part 2, 447–450, 18-21 Sept. 1984.

[4] J.A.A. Melkebeek and J.L. Willems, Reciprocity relations for the mutual inductances between orthogonal axis windings in saturated salient-pole machines, *IEEE Trans. on Industry Applications*, (26), 107–114, Jan./Feb. 1990.

[5] D.W. Novotny and T.A. Lipo, *Vector control and dynamics of AC drives*, (1st ed.), Clarendon Press, Oxford, 1996.

[6] H. Polinder and M.J. Hoeijmakers, Eddy-current losses in segmented surface-mounted magnets of a PM machine, *IEE Proc.-Electr. Power Appl.*, (146), 261–266, May 1999.